Infrared Spectroscopic and Density Functional Theoretical Investigation of the Reaction Products of Laser-Ablated Zr, Hf, and Th Atoms with Nitric Oxide

Gary P. Kushto and Lester Andrews*

Department of Chemistry, University of Virginia, Charlottesville, Virginia

Received: February 16, 1999; In Final Form: April 12, 1999

Laser-ablated Zr, Hf, and Th atoms react with NO to form the bent NMO insertion products. These favorable reactions proceed on annealing to 21−24 K. The NMO molecules are characterized by isotopic substitution and M−O stretching modes at 844.2, 855.2, and 760.3 cm^{-1} and M−N stretching modes at 673.3, 685.3, and 697.3 cm^{-1}, respectively. The increase in bond stretching frequencies from Zr to Hf is due to relativistic contraction not found from Hf to Th. The BP86 functional and averaged relativistic effective potentials for Zr and Hf predict bent $^2A'$ states and observed frequencies within 1−3% and the isotopic shifts within 2 cm^{-1}.

Introduction

Nitric oxide is a common pollutant molecule, and it is important to understand the role of metals in the reduction of NO.[1] Furthermore, NO has played a central role in traditional coordination chemistry.[2,3] Both carbon monoxide and nitric oxide have been used as infrared spectral probes in the study of structures of coordination complexes. Nitric oxide has also been found in chemical systems that have significant biological and environmental implications. In biology, NO is well-known to bind to the heme center in numerous metalloproteins as a protective step in the defense against system toxins.[4] In a somewhat analogous manner, NO acts as a powerful bioregualtor in several heme-containing enzymatic cycles. Also, NO has recently been identified as an important messenger molecule in neurophysical systems.[6,7] Because NO is a primary byproduct in the combustion of fossil fuels, understanding its atmospheric chemistry is important; therefore, reactions of NO with atmospheric components such as ozone[8] may provide new information to minimize pollution of this type. In addition to the atmospheric chemistry of NO, it is important to understand the interactions of NO with any number of transition metals and transition metal surfaces because these catalytic materials are finding widespread use in industry for the removal of NO and other ozone-depleting gases from industrial effluent.[9]

To gain a better understanding of the reactions of transition metals with NO, we have undertaken a series of experiments designed to investigate the molecular species produced by the reactions of NO with laser-ablated transition metals.[10−15] The current study, and a closely related previous investigation with titanium,[15] focuses on the products of the group IV metal atom reactions with NO. The group IV metals (Ti, Zr, and Hf) are an ideal subject for the study of systems of this nature because their chemistries have been thoroughly examined primarily because of their role as the basis of the Ziegler−Natta polyolefin catalysts.[2,3] In the present investigation, the heavier metal atoms of group IV (Zr, Hf, and the pseudo group IV metal Th) are studied to evaluate their possible utility as nitric oxide activation catalysts.

In addition to the importance of these metals as catalytic centers, from a systematic investigation into the full group, the results of relativistic effects on the bonding in these closely related systems can be evaluated. This is most important in the products formed by thorium. Reactions of laser-ablated thorium atoms with H_2, O_2, and N_2[16−18] have provided the triatomic insertion products HThH, OThO, and NThN; however, it has been determined through theoretical modeling that the roles of the metal orbitals in the bonding of these species are significantly different from that of the related uranium analogues. These differences arise from several interplaying factors, but the largest contributors to these chemical differences are the second-order relativistic effects on the relative energies and radial extents of the 5d and 4f orbitals of the thorium and uranium centers.[19−21] These relativistic effects are of significant interest to the theoretical community,[19−21] and a more complete understanding of the latter can only be effected by evaluation of the accuracy of the results of new theoretical models versus available experimental data. For the purposes of characterizing such molecular species, we include infrared spectroscopic investigation of the reaction products of laser-ablated thorium atoms and NO.

Experimental Section

The vacuum system and cryogenic chamber for Nd:YAG laser ablation has been described previously.[22,23] The CsI spectroscopic window was maintained at 6−7 K by an APD Cryogenics closed-cycle refrigerator. Absolute temperatures were measured by a Au/Co versus chromel thermocouple. Vapor-phase zirconium, hafnium, and thorium atoms were produced by focusing the 1064 nm fundamental of a Q-switched Spectra Physics Quanta Ray DCR-11 Nd:YAG laser onto the respective polished metal targets. The average laser pulse duration was set at 10 ns, and the laser power at the target was varied between 10 and 50 mJ/pulse with a 10 Hz repetition rate. The zirconium, hafnium (Johnson-Matthey, lump, 99%), and thorium (Oak Ridge National Laboratory, 99%) metal targets were mounted on a rotating (1 rpm) metal rod to avoid laser pitting of the target surface. The nitric oxide samples were prepared in molar ratios ranging from Ar/NO = 100:1 to 500:1 in order to evaluate the effect of nitric oxide concentration on the formation of each of the products. Isotopically mixed samples ($^{14}N^{16}O/^{15}N^{16}O$,

10.1021/jp9905732 CCC: $18.00
Published on Web 06/06/1999

$^{15}N^{16}O/^{15}N^{18}O$, and $^{14}N^{16}O/^{14}N^{18}O/^{15}N^{16}O/^{15}N^{18}O$) were also employed. The average co-deposition of the metals and Ar/NO sample lasted 1−2 h with the gas spray on rate between 3 and 5 mmol/h.

Infrared spectra were recorded on a Nicolet 550 spectrometer bench operating with a spectral resolution of 0.5 cm^{-1} and a frequency accuracy of 0.1 cm^{-1}. Spectra were collected at the end of each deposition and before and after annealings or photolyses. Typically, each matrix was annealed quickly to 25, 30, 35, and 40 K. Broadband mercury arc photolysis using a medium-pressure mercury arc lamp (Philips H39KB) with the outside globe removed (240−580 nm) was performed at different points in the course of the experiments.

Computational Methods

Density functional theory (DFT) based calculations were performed using the Gaussian 94 suite of programs.[24] The exchange and correlation functionals of Becke[25] and Perdew (BP86),[26] respectively, were used throughout and provided results that matched experimentally observed vibrational frequencies and relative spectral intensities exceptionally well. The nitrogen and oxygen atoms were treated with the 6-31+G* all-electron basis, while the zirconium and hafnium atoms were described using the averaged relativistic effective potentials (AREP's) and the complementary basis sets due to LaJohn et al.[27] and Ross et al.,[28] respectively. The zirconium and hafnium basis sets were the (5s 5p 4d) minimal basis sets optimized for use with the AREP's mentioned above. These basis sets were completely uncontracted ([11111/11111/1111]) for optimal flexibility in the valence region and in order to avoid the errant basis set contraction borne problems observed for similar sets in previous studies.[29] The near orbital degeneracy of the 5s and 5p orbitals in the zirconium set[30] was accounted for by the addition of two p type functions and a single d type basis function that were nonenergy-optimized and generated in the manner outlined in the manuscript by Wittborn and Wahlgren.[31] The two additional p type functions added to the zirconium set were given the same exponential value as the two most diffuse s type functions in the minimal basis. The additional d type function was given an exponential factor equal to that of the outermost d type function scaled by the ratio of the exponential factors of the outermost and the next outermost d type functions. The addition of the above basis set augmentations tended to aid in the convergence of the often troublesome SCF wave functions associated with zirconium-containing species. The hafnium basis set was used as taken from the literature.[28]

Results

The reactions of laser-ablated zirconium, hafnium, and thorium atoms with nitric oxide in excess argon were examined using a range of laser powers, NO concentrations, and isotopic modifications. Infrared spectra in the metal oxide and nitride stretching regions are contrasted for Ti, Zr, Hf, and Th with $^{14}N^{16}O$ in Figure 1 to show the effects of shell expansion and relativistic contraction.[32] Figure 2 illustrates the annealing and photolysis behavior for the Zr/NO solid argon system. Figures 3−5 show spectra of the reaction products of Zr, Hf, and Th with mixed isotopic nitric oxide reagents. Complete lists of all product absorptions in solid argon are given in Tables 1, 2, and 3 for the Zr, Hf, and Th reactions with NO, respectively. For the sake of brevity, even though absorptions due to N_2O, NO_2, $(NO)_2^+$, NO_2^-, and both of the $(NO)_2^-$ species[12] are observed in the spectra of all of the metal reactions, they are only listed in Table 1.

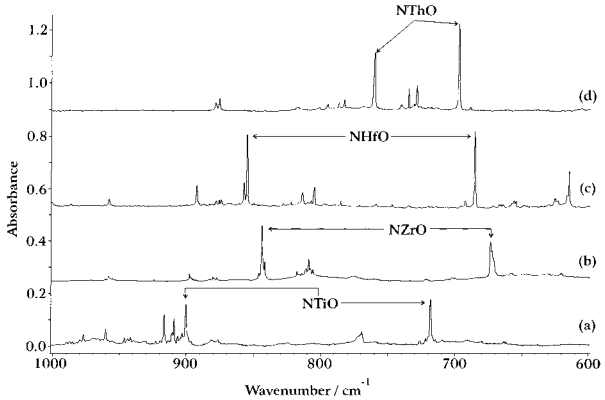

Figure 1. Infrared spectra in the 1000−600 cm^{-1} region for the reaction products of laser-ablated Ti, Zr, Hf, and Th atoms with argon/$^{15}N^{16}O$ (500:1) samples following 2 h of co-deposition and matrix annealing to 21−24 K: (a) Ti, (b) Zr, (c) Hf, and (d) Th.

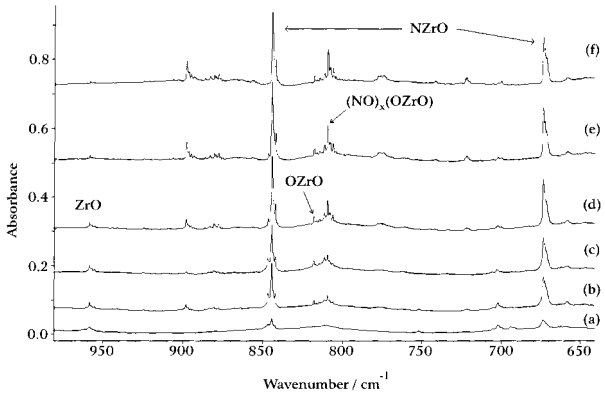

Figure 2. Infrared spectra in the 980−640 cm^{-1} Zr−N and Zr−O stretching region for laser-ablated Zr atoms with an argon/$^{14}N^{16}O$ (500:1) sample (a) following 2 h of co-deposition, (b) after annealing to 24 K, (c) following a 45 min broad-band Hg arc photolysis, (d) after annealing to 30 K, (e) to 35 K, and (f) to 40 K.

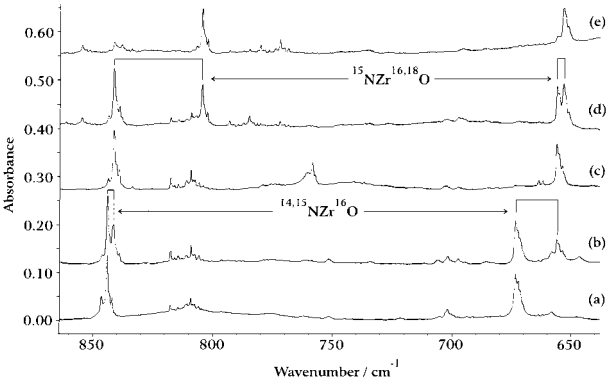

Figure 3. Infrared spectra in the 860−640 cm^{-1} Zr−N and Zr−O stretching region for laser-ablated Zr atoms with (a) argon/$^{14}N^{16}O$ (500:1) sample, (b) argon/$^{14}N^{16}O$/ $^{15}N^{16}O$ (1000:1:1) sample, (c) argon/$^{15}N^{16}O$ (500:1) sample, (d) argon/$^{15}N^{16}O$/ $^{15}N^{18}O$ (1000:1:1), and (e) argon/$^{15}N^{18}O$ (500:1) sample. All spectra were taken of matrices following 1−4 h of co-deposition and annealing to 32−34 K.

The results of the density functional theory calculations for the Zr and Hf + NO product species (electronic state term symbol, total energy, and harmonic vibrational frequencies) are presented in Table 4, and the DFT optimized geometries are shown pictorially in Figure 6, which includes Ti for comparison.[15,33]

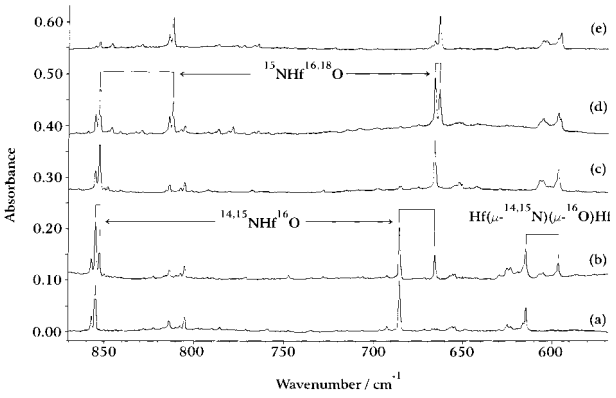

Figure 4. Infrared spectra in the 870−570 cm^{-1} Hf−N and Hf−O stretching region for laser-ablated Hf atoms with (a) argon/$^{14}N^{16}O$ (500:1) sample, (b) argon/$^{14}N^{16}O/^{15}N^{16}O$ (1000:1:1) sample, (c) argon/$^{15}N^{16}O$ (500:1) sample, (d) argon/$^{14}N^{16}O/^{15}N^{16}O/^{14}N^{18}O/^{15}N^{18}O$ (4000:1:1:1:1) sample, and (e) argon/$^{15}N^{18}O$ (500:1) sample. All spectra were taken of matrices following 2−4 h of co-deposition and annealing to 30−32 K.

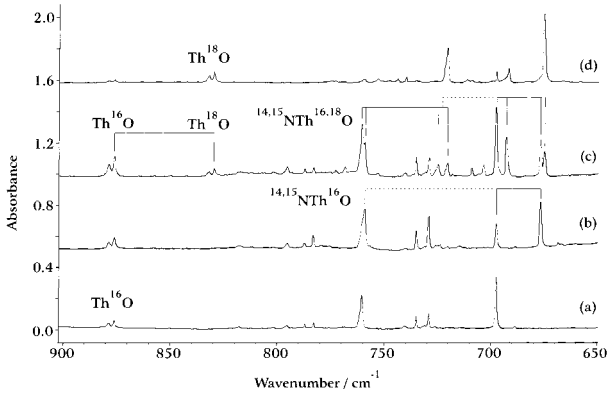

Figure 5. Infrared spectra in the 900−650 cm^{-1} Th−N and Th−O stretching region for laser-ablated Th atoms with NO samples: (a) Th + argon/$^{14}N^{16}O$ (300:1); (b) Th + argon/$^{14}N^{16}O/^{15}N^{16}O$ (600:1:1); (c) Th + argon/$^{15}N^{16}O$ (300:1); (d) Th + argon/$^{14}N^{16}O/^{15}N^{16}O/^{14}N^{18}O/^{15}N^{18}O$ (1200:1:1:1:1). All spectra were taken after 1.5 h of metal−nitric oxide co-deposition.

Discussion

The above product absorptions will be assigned in the ensuing discussion on the basis of isotopic shifts and splittings, as well as by analogy with density functional calculations on suspected product species. Assignments for each of the product absorptions are also listed in Tables 1−3.

NZrO. Because they are isovalent and known to exhibit similar reactivity patterns in conventional chemistry, the primary reaction product in the Zr + NO system should be the analogue of the previously observed Ti insertion product NTiO.[15] In the infrared spectrum of the reaction products of laser-ablated zirconium atoms with Ar/$^{14}N^{16}O$, the two weak absorptions at 844.2 and 673.3 cm^{-1} (Figure 2) that increase in intensity by a factor of 4 upon 24 K annealing provide evidence for the formation of the NZrO insertion product with little activation energy requirement, as also found for Ti.[15] These vibrations exhibit mechanics consistent with nearly isolated terminal Zr−O and Zr−N bonds, respectively. Upon isotopic substitution with ^{15}NO, the lower frequency mode red-shifts to 655.6 cm^{-1}, producing a $^{14}N/^{15}N$ isotope ratio of 1.027 00 (Figure 3), which is close to but less than the Zr−N diatomic value of 1.030 06. This band undergoes a further red shift in the reactions with $^{15}N^{18}O$ to 653.0 cm^{-1}, indicating a slight but distinct frequency dependence on the mass of the oxygen atom. The higher frequency mode of this set shows complementary behavior by shifting slightly to the red in the $^{15}N^{16}O$ experiments (841.5 cm^{-1}) and exhibiting a large ^{18}O shift to 804.7 cm^{-1} ($^{16}O/^{18}O$ = 1.045 73) justifying assignment of this absorption to a primarily Zr−O vibration. Reactions of zirconium atoms with isotopically mixed NO samples ($^{14}N^{16}O/^{15}N^{16}O$, $^{15}N^{16}O/^{15}N^{18}O$, and $^{14}N^{16}O/^{15}N^{16}O/\ ^{14}N^{18}O/^{15}N^{18}O$) provide spectroscopic evidence that this species incorporates one NO subunit; namely, the upper band shows a doublet (841.5−804.7 cm^{-1}) in the $^{15}N^{16}O/^{15}N^{18}O$ experiments, the lower band appears as a doublet (673.3−655.6 cm^{-1}) in the mixed $^{14}N^{16}O/^{15}N^{16}O$ experiments, and each of the two absorptions splits into a quartet with the isotopically randomized precursor (844.2−841.5−808.6−804.8 cm^{-1} and 673.3−669.4−655.6−653.0 cm^{-1}). The analogous NTiO product exhibited resolved ^{n}Ti isotopes for a single Ti atom species.[15] These spectra provide a complete set of data for assignment of the 844.2 and 673.3 cm^{-1} absorptions to the NZrO molecule.

Further support for identification of the NZrO molecule comes from DFT calculations. The BP86/AREP method predicts a $^2A'$ electronic ground state for NZrO, which is similar to that found for the NTiO species.[15] As with NTiO, NZrO has a bent structure with an apex angle of 103.3°, indicating that the bonding in this molecule is primarily d orbital in character. The calculated frequencies of 853 and 686 cm^{-1} for the primarily Zr−O and Zr−N stretching modes also match the experimentally observed values of 844.2 and 673.3 cm^{-1} within 1%. In addition to the frequency match, the theoretically derived force field for NZrO reproduces the isotope shifts to within an average of 2 cm^{-1}, further supporting the assignment of these bands to the NZrO insertion product.

NHfO. As with the zirconium (and titanium) analogue discussed above, the NHfO molecule is formed readily by the reaction of hafnium atoms with Ar/NO mixtures even on annealing to 21 K in solid argon. In the Hf + $^{14}N^{16}O$ spectra, the bands at 855.2 and 685.3 cm^{-1} are indicative of the formation of the NHfO species (Figure 1c). In a manner consistent with the other metals of group IV, the lower frequency band due to the NHfO molecule can be associated with the primarily Hf−N stretching motion, exhibiting a 19.6 cm^{-1} $^{15}N^{16}O$ isotope shift ($^{14}N/^{15}N$ = 1.029 44 isotope ratio) while showing only a 2.7 cm^{-1} red shift as a result of $^{15}N^{18}O$ isotope labeling. In a complementary fashion, the higher frequency mode exhibits vibrational mechanics consistent with a primarily Hf−O mode, showing a 41.0 cm^{-1} dependence on the mass of the oxygen atom ($^{16}O/^{18}O$ = 1.050 62 isotope ratio) and only a 2.2 cm^{-1} red shift due to ^{15}N isotopic substitution. In the isotopically mixed experiments, these bands are split in a manner consistent with the vibrations of two slightly coupled, terminal stretching Hf−N and Hf−O coordinates. These splittings are best displayed in the randomized $^{14}N^{16}O/^{15}N^{16}O/^{14}N^{18}O/^{15}N^{18}O$ experiments (Figure 4) where the primarily Hf−O motion splits into a quartet of bands located at 855.2−853.0−815.2−812.0 cm^{-1} and the lower frequency Hf−N type motion splits into a similar quartet located at 685.3−681.6−665.7−663.0 cm^{-1}. This complete set of absorptions provides strong support for the assignment of these bands to the NHfO molecular insertion product.

BP86/AREP calculations on the NHfO species predict the ground-state $^2A'$ species to be bent, much like the Ti and Zr species, with an N−Hf−O apex angle of 102.2°. The theoretically derived vibrational force field for this species models frequencies (within 0.4 and 2.6%) and the isotopic shifts (and hence vibrational mode mixing) exceptionally well (isotopic

TABLE 1: Observed Vibrational Frequencies (cm^{-1}) for Matrix-Isolated Species Produced by Reactions of Laser-Ablated Zirconium Atoms with Nitric Oxide Diluted in Argon

products	$^{14}N^{16}O$	$^{14}N^{16}O + {}^{15}N^{16}O$	$^{15}N^{16}O$	$^{15}N^{16}O + {}^{15}N^{18}O$	$^{15}N^{18}O$
(NNO)(ZrO)	2295.6	2295.6−2273.3−2247.2−2224.8	2224.8	2224.8−2216.4	2216.4
NNO	2218.4	2218.4−2196.3-2172.4−2149.5	2149.5	2149.5-	- -
NO	1871.7	1871.7−1838.7	1838.7	1838.7−1789.2	1789.2
$(NO)_2$	1863.2	1863.2−1849.6−1830.4	1830.4	1830.4−1812.0−1781.2	1781.2
$(NO)_2$	1776.1	1776.1−1757.5−1744.6	1744.6	1744.6−1714.7−1697.4	1697.4
NO_2	1610.8	1610.8−1576.1	1576.1		1545.7
$Zr(NO)_x$	1598.7				1533.9
$[(NO)_2]^+$	1589.1	1589.1−1574.9−1561.8	1561.8	1561.8−1539.9−1520.2	1520.3
$[(NO)_2]^+$ (site)	1581.3	1583.1−1569.8−1555.8	1555.8	1555.8−1533.9−1514.5	1514.5
$Zr(NO)_x$	1567.7		1540.2		1500.2
$Zr(NO)_x$	1530.9		1497.6		1462.4
$OZr-\eta^2-(N_2O)$	1447.2	1447.2−1440.3−1415.7−1408.7	1408.7	1408.7−1393.7	1393.7
$OZr-\eta^2-(N_2O)$	1213.7	1213.7−1199.1−1196.9−1181.9	1181.9	1181.9−1167.6	1167.6
ZrO	958.7	958.7	958.7	958.7−912.5	912.5
$OZr-\eta^2-(N_2O)$	897.8	897.8	897.8	897.8−855.0	855.0
NZrO	844.2	844.2−841.5	841.5	841.5−804.7	804.7
OZrO, ν_3	817.8	817.8	817.8	817.8−793.1−780.3	780.3
(N_2)OZrO, "ν_3"	809.2	809.2	809.2	809.2−784.9−772.1	772.1
NZrO	673.3	673.3−655.6	655.6	655.6−653.0	653.0

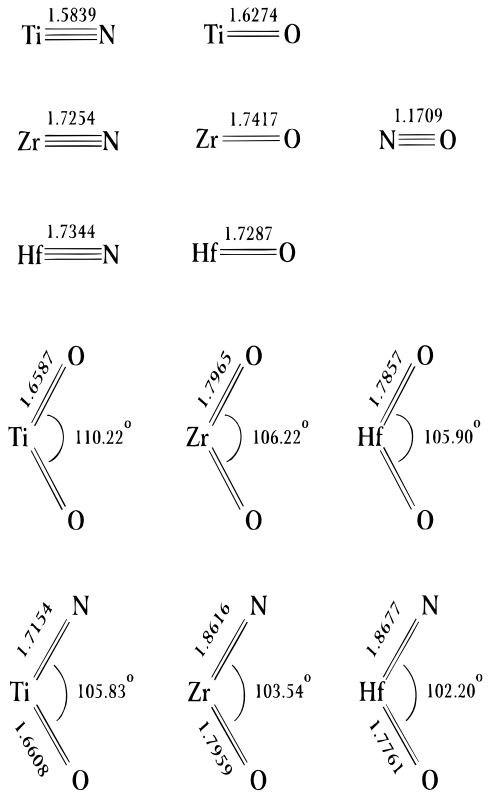

Figure 6. Calculated density functional geometries of the species produced by the reactions of laser-ablated Ti (BP86/Watchers+spd), Zr (BP86/AREP), and Hf (BP86/AREP) atoms with nitric oxide. All bond lengths are quoted in angstroms, and bond angles are given in degrees.

shifts within 0.5−1.2 cm^{-1}), providing further support for the assignment of the above bands to NHfO species.

NThO. A recent investigation of the Th + N_2 system found that laser-ablated thorium atoms insert into the N−N bond of dinitrogen to form the linear molecule NThN.[18] This geometric form is in stark contrast to the bent OThO species,[17] a dichotomy that was explained by differences in the relative energies of the O 2p, the N 2p, and the Th 5f orbitals.[21,32] The present investigation of the Th + NO system has provided spectral data on the molecular system chemically intermediate between the linear NThN and the bent OThO molecules, NThO. In the Th + $^{14}N^{16}O$ experiments, the infrared spectra (Figure 1d) contain two weak features that grow by a factor of 4 on annealing the matrix to 23 K that are due to the NThO species. Such growth in the cold matrix environment provides evidence that the direct insertion reaction, Th into the N−O bond, requires little or no activation energy, which is an interesting result in its own right. The lower frequency absorption of the pair noted above, which appears at 697.3 cm^{-1} in the Th + $^{14}N^{16}O$ experiments, can be attributed to the Th−N stretching vibration of this species on the basis of the high $^{14}N/^{15}N$ isotope ratio (1.039 00) that this mode exhibits upon isotopic substitution at the nitrogen center. As with the NZrO and NHfO species, this mode is coupled very slightly to the M−O stretching coordinate, showing a 1.7 cm^{-1} dependence on the mass of the oxygen nucleus. In a complementary fashion, the primarily Th−O stretch of this molecule, which occurs at 760.3 cm^{-1} in the Th + $^{14}N^{16}O$ experiment, exhibits little dependence on the mass of the nitrogen red-shifting 1.3 cm^{-1} to 759.0 cm^{-1} in the $^{15}N^{16}O$ experiments. This mode exhibits a nearly diatomic ThO $^{16}O/^{18}O$ ratio of 1.053 73, further supporting the Th−O stretching nature of this vibration.

The NThO stoichiometry of this species is confirmed by the reactions of the laser-ablated thorium atoms with mixtures of isotopically labeled nitric oxide: $^{14}N^{16}O/^{15}N^{16}O$ and $^{15}N^{16}O/^{15}N^{18}O$. In the mixed nitrogen isotope experiments, the lower frequency band splits into a doublet at 697.3−676.4 cm^{-1} and the higher frequency absorption broadens and red-shifts slightly to 759.2 cm^{-1} (Figure 5), which is consistent with the vibration of a single nitrogen atom. The reactions of Th with mixed oxygen isotopic samples provide analogous data in which the absorption due to the primarily Th−O vibration appears as a doublet at 759.0−720.3 cm^{-1} and the lower frequency absorption splits into a very closely spaced doublet at 676.4−674.7 (Figure 5), demonstrating that a single oxygen atom participates in these vibrations. All of the above data confirm assignment of these absorptions to the Th−N and Th−O stretching vibrations of the NThO species. Finally, this assignment is supported by quasi-relativistic density functional calculations,[16,33] which predict a bent $^2A'$ NThO molecule with strong infrared absorptions at 777 and 712 cm^{-1}.

Now that a complete set of data on OThO, NThO, and NThN has been collected, it is interesting to note some of the more qualitative differences (or similarities) among these actinide-containing species. First, the Th−O stretching frequency of NThO (760.3 cm^{-1}) lies almost at the average of the ν_1 and ν_3 modes of OThO, indicating that the Th−O bond orders of these

TABLE 2: Observed Vibrational Frequencies (cm^{-1}) for Matrix-Isolated Species Produced by Reactions of Laser-Ablated Hafnium Atoms with Nitric Oxide Diluted in Argon

products	$^{14}N^{16}O$	$^{14}N^{16}O + {}^{15}N^{16}O$	$^{15}N^{16}O$	$^{15}N^{16}O + {}^{15}N^{18}O$	$^{15}N^{18}O$
(NNO)(HfO)	2303.6	2303.6−2282.8−2255.1−2232.5	2232.5	2232.5−2224.4	2224.1
$Hf(NO)_x$	1594.4		1566.5		1524.4
$Hf(NO)_x$	1565.2		1537.4		1496.7
$Hf(NO)_x$	1519.7		1490.2		1461.2
OHf−η^2-(N_2O)	1437.3	1437.3−1433.9−1406.4−1402.5	1402.5	1402.5−1382.2	1382.2
OHf−η^2-(N_2O)	1202.8	1202.8−1189.9−1177.9−1168.4	1168.4	1168.8−1158.7	1158.7
HfO	958.4	958.4	958.4	958.4−908.3	908.3
OHf−η^2-(N_2O)	892.6	892.6	892.6	892.6−846.3	846.3
NHfO	855.2	855.2−853.0	853.0	853.0−812.0	812.0
OHfO, ν_3	814.0	814.0	814.0	814.0−786.4−772.2	772.2
(N_2)OHfO, "ν_3"	805.3	805.3	805.3	805.3−778.5−764.4	764.4
NHfO	685.3	685.3−665.7	665.7	665.7−663.0	663.0
Hf(μ-N)(μ-O)Hf	654.3	654.3−652.1	652.1	652.1−623.2	623.2
Hf(μ-N)(μ-O)Hf	614.5	614.5−596.3	596.3	596.3−594.7	594.7
Hf(μ-N)(μ-O)Hf	495.0	495.0−494.3	494.3	494.3−469.7	469.7

TABLE 3: Observed Vibrational Frequencies (cm^{-1}) for Matrix-Isolated Species Produced by Reactions of Laser-Ablated Thorium Atoms with Nitric Oxide Diluted in Argon

products	$^{14}N^{16}O$	$^{14}N^{16}O + {}^{15}N^{16}O$	$^{15}N^{16}O$	$^{15}N^{16}O + {}^{15}N^{18}O$	$^{15}N^{18}O$
(NNO)(ThO)	2265		2194		2186
(NNO)(ThO)	2240		2170		2163
OTh−η^2-(N_2O)	1389.9	1389.9−1386.6−1360.2−1356.3	1356.3	1356.3−1335.9	1335.9
OTh−η^2-(N_2O)	1165.7	1165.7−1161.0−1140.7−1136.9	1136.9	1136.9−1117.8	1117.8
ThN	934.5	934.5−904.7	904.7	904.7	904.7
ThO	878.8	878.8	878.8	878.8−831.9	831.9
ThO (site)	876.3	876.3	876.3	876.3−829.6	829.6
OTh−η^2-(N_2O)	817.7	817.7	817.7	817.7−774.7	774.7
(NNO)(ThO)	795.3	795.3	795.3	795.3−752.9	752.9
OThO, ν_1	787.3	787.3	787.3	787.3−772.7−743.78	743.8
(N_2)OThO, "ν_1"	783.2	783.2	783.2	783.2−768.3−739.8	739.8
NThO	760.3	759.2	758.7	758.7−720.3	720.3
OThO, ν_3	735.0	735.0	735.0	735.0−708.8−697.1	697.1
(N_2)OThO, "ν_3"	729.0	729.0	729.0	729.0−703.2−691.4	691.4
NThO	697.3	697.3−676.4	676.4	676.4−674.7	674.7

two species are close to being equivalent. On the other side of the molecule, the Th−N stretching frequency occurs at 697.3 cm^{-1}, which is significantly lower than the Th−N stretching vibrations[18] of NThN, indicating that the Th−N bond of NThO is of a somewhat lower order than the Th−N bonds in NThN, presumably due to unfavorable competition with O for the Th valence electron density. The angle calculated for NThO (127.1°) using DFT is between the angles for OThO (117.7°) and NThN (180°), and the larger valence angle in NThO relative to OThO can, to some extent, be explained by an increase in the contribution of Th 5f orbitals.[33] In a very qualitative analysis it certainly appears that the bonding in the NThO molecule is more similar to that in the OThO species than to that in NThN. In effect, in the dioxygen and nitric oxide systems, thorium behaves more like a transition metal in that the bonding in these systems is almost purely 6d in nature. This is in contrast to the NThN species in which the high symmetry and increased 5f orbital participation in the bonding (as a result of the relative energy of the nitrogen 2p orbitals versus the analogous orbitals of oxygen) allow thorium to behave more like one of the actinide metals.[18]

OM−*N,N*-η^2-(N_2O) (M = Ti, Zr, Hf, and Th). Annealing increases bands at 1863.2 and 1776.1 cm^{-1} at the expense of the strong $^{14}N^{16}O$ band at 1871.7 cm^{-1}, which demonstrates dimerization of the NO diatomic molecule. As the matrix is annealed and nitric oxide dimerizes, the importance of monomer chemistry begins to decline and the chemistry of $(NO)_2$ is expected to become much more prevalent. Therefore, reaction products of dimer species with the diffusing transition metal atoms must be considered. In the experiments with each of the metals, bands grow in on matrix annealing that can be associated with metal reactions with NO dimer or two successive NO molecules. These products are typified by three absorptions: one in the 1500−1450 cm^{-1} region, one in the 1200−1150 cm^{-1} region, and one in the M−O stretching regions for the metal involved. In the reactions of Zr with $^{14}N^{16}O$, bands at 1447.2, 1213.7, and 897.8 cm^{-1} (Table 1) all share similar annealing and photolysis behaviors and can be associated with vibrations of the same molecular species. These bands are very weak or unobserved on deposition but grow in markedly on warming of the matrix, reaching their maximum intensity upon the highest temperature annealings. In addition, the species giving rise to these bands is photosensitive, as indicated by the disappearance of all three bands on broadband photolysis. Such drastic photolytic behavior makes grouping these three bands as being due to the same species straightforward. In addition to analogous features in the Ti + NO spectra,[15] absorptions exhibiting analogous annealing and photolysis behaviors are observed in the Hf + $^{14}N^{16}O$ spectra at 1437.2, 1202.8, and 892.5 cm^{-1} (Table 2) and in the Th + $^{14}N^{16}O$ spectra at 1389.9, 1165.7, and 817.7 cm^{-1} (Table 3).

In the reactions of each metal with a $^{14}N^{16}O/^{15}N^{16}O$ mixture, the highest and middle frequency bands of each set split into a quartet, indicating that both vibrations arise from the motions of two symmetry-inequivalent nitrogen atoms. The relatively large $^{14}N/^{15}N$ isotope ratios exhibited by these modes also indicate that these are primarily N−N stretching coordinates: Ti, 1488.8/1448.7 = 1.027 47 and 1208.8/1178.8 = 1.025 45;[15,33] Zr, 1447.2/1408.7 = 1.02733 and 1213.7/1181.9 = 1.026 91; Hf, 1437.3/1402.5 = 1.024 81 and 1202.8/1168.4 = 1.029 44; Th, 1389.9/1365.3 =1.024 77 and 1165.7/1136.9 =1.025 33). In addition to the large nitrogen isotopic shift associated with

these modes, there is a distinct oxygen isotope dependence in these vibrations as evidenced by the fact that these absorptions appear as doublets in the mixed $^{15}N^{16}O/^{15}N^{18}O$ experiments (Tables 1−3). The above isotope splittings provide evidence that these bands are produced by a molecular subunit of the stoichiometry N_2O. It is also interesting to note that since the frequencies of these bands are relatively invariant among the Zr, Hf, and Th experiments, it is reasonable to believe that the chromophore giving rise to these absorptions is relatively robust, which is consistent with a coordinated nitrous oxide molecule. The most striking thing about the vibrational spectra of these species is the frequency region for the N−N stretch. In uncomplexed N_2O, the N−N stretching motion occurs at 2218.2 cm^{-1} in solid argon, but in the present species, this mode drops into the high 1400 cm^{-1} region and mixes with the associated N−O vibration of this NNO unit. This type of reduction in the strength of an N−N bond is consistent with an η^2-bound N−N complex, as has been observed in the reactions of the early transition metals with dinitrogen.[34−38] From this information it is reasonable to believe that these absorptions arise from a nitrous oxide complex η^2-bound to a Zr, Hf, or Th center through the N−N bond with the remaining oxygen atom pointed away from the transition metal center in a manner consistent with the observed and calculated Ti analogue OTi−η^2-(N_2O).[15]

The third absorption due to this molecule can be characterized as a pure M−O stretching vibration. In none of the group IV metal experiments with a mixed $^{14}N^{16}O/^{15}N^{16}O$ sample do these absorptions show a perceptible dependence on the nitrogen isotopic mass; however, as would be expected for a pure, terminal M−O stretching mode, these vibrations do produce doublets in the $^{15}N^{16}O/^{15}N^{18}O$ experiments and exhibit nearly pure $M^{16}O/M^{18}O$ diatomic isotope ratios (Tables 1−3). With the assignment of these latter bands, it is evident that the species giving rise to both the N_2O and M−O type vibrations are nitrous oxide complexes of the group IV metal monoxides. As mentioned above, the low energy of the N−N stretching mode of this species suggests that the NNO subunit of this complex is η^2-bound to the metal monoxide through the N−N bond and that this bond is readily reduced by the metal monoxide, suggesting the possible importance of the group IV metals and metal oxides as N−N bond activation catalysts.

The simplest way to synthesize a species of the nature described above is to react laser-ablated metal atoms with nitrous oxide to produce the obvious products: the metal monoxide and dinitrogen. This newly formed MO product could then go on to react with a second nitrous oxide molecule to form the OM−η^2-(N_2O) complex; however, this is not observed. In the reactions of the early transition metals (and thorium) with N_2O, the only products observed are the metal oxides and their analogous dinitrogen complexes. This suggests that the OM−η^2-(N_2O) complex can only be formed by species present in the NO experiments, most likely $(NO)_2$. It is postulated that this species is formed by the insertion of a cold transition metal atom into one of the O−N bonds of the dimer upon matrix annealing. This reaction is most likely exothermic enough to drive the rearrangement of this intermediate (OMNNO) to the observed, η^2-bound species in the cold matrix environment. Alternatively, a second NO could add to the bent NMO product. Our BP86 calculations indicate that the side-bound species is significantly more stable than any of the calculated η^1-bound conformers for titanium,[15] supporting the current mechanistic argument and the overall assignment of these species.

Other Metal−$(NO)_2$ Reaction Products. Apart from the OM−η^2-(N_2)O species mentioned above, there are several other species formed exclusively in the M + NO systems that can be associated with higher order metal reactions such as with NO dimer or multiple NO molecules. In the spectra of Zr, Hf, and Th with NO, bands grow in on annealing at 2295.6, 2303.6, and 2265−2240 cm^{-1}, respectively, that provide evidence for a perturbed N_2O type of species. In the spectra of each metal reacted with a $^{14}N^{16}O/^{15}N^{16}O$ mixture, each of the above absorptions splits into 1:1:1:1 relative intensity quartet, indicating that these modes are produced by the vibrations of two symmetry-inequivalent nitrogen atoms (Tables 1−3). In the mixed $^{15}N^{16}O/^{15}N^{18}O$ experiments, these modes appear as doublets, suggesting strongly that these absorptions arise from a chromophore of the stoichiometry NNO. The frequency region that these modes occupy also suggests an unusual mode of ligation for this NNO ligand, since complexation of a traditional geometry (through the N−N unit) would tend to weaken the N−N bond as noted above in the discussion on OM−η^2-(N_2)O. In contrast, the observed data suggest that this N_2O fragment is coordinated to a metal center through the oxygen atom. A coordination of this nature would weaken the N−O bond of N_2O, forcing the N−N vibrational frequency blue toward the value of free dinitrogen. The absence of absorptions due to this species in the M + N_2O experiments indicates that the parentage of this species does not involve the naked metal and the N_2O molecule; therefore, these molecules are more likely the product of metal−$(NO)_2$ reactions. Tentatively, these absorptions are assigned to the complex OM−ONN.

In the M−O stretching region, bands that exhibit no nitrogen isotope shift and split into triplets in the mixed $^{15}N^{16}O/^{15}N^{18}O$ experiment provide evidence for the formation of group IV (N_2)-(MO_2) complexes. Although the formation of such species in the present system might result from atmospheric contaminants, the observation of $M^{18}O_2$ counterparts from the $^{15}N^{18}O$ reaction provides strong evidence that these absorptions are the result of metal atom reactions with NO dimer or two successive NO molecules. The bands observed at 909.3 cm^{-1} in the Ti + $^{14}N^{16}O$ and 909.3−882.3−874.3 cm^{-1} in the mixed $^{15}N^{16}O/^{15}N^{18}O$ experiments[15] are identical to the bands observed in $Ti/O_2/N_2/Ar$ mixtures and are assigned to a dinitrogen complex of OTiO.[39] This result suggests that the present absorptions in the Ti, Zr, and Hf systems are due to the same species and not to possible nitrosyl complexes of the metal dioxides. Although no associated N−N stretching fundamental was observed for the titanium species in the previous[15] or present studies, important comparisons can be drawn between the systems at hand and the results of recent studies of the reactions of V, Nb, and Ta with NO. In these systems, strong bands grew in upon annealing in the N−N and M−O stretching regions that showed identical photolytic and annealing behaviors and isotopic dependencies consistent with a dinitrogen complex of the metal dioxides.[13,14] From this evidence, it is suggested that the features in the Ti−O, Zr−O, and Hf−O stretching regions are the result of the reaction with two NO molecules to form dinitrogen and the metal dioxide. The resulting dinitrogen complex is most certainly η^2-bound, which accounts for the absence of a strong N−N stretching absorption in the high 2100 cm^{-1} region. Previous DFT calculations[15] provide further support for this species by suggesting that the (N_2)(OTiO) complex is by far the most stable of all possible conformers of the stoichiometry TiN_2O_2.

Hf(μ-N)(μ-O)Hf. In addition to the intense absorptions in the spectra of the reaction products of M + NO that are due to the metal insertion product, there is an additional set of bands in the hafnium experiment that has no obvious analogue in the titanium or zirconium systems. These bands occur at 654.3,

TABLE 4: Density Functional (BP86/AREP) Energies and Harmonic Vibrational Frequencies (cm^{-1}) for Products of the Zirconium and Hafnium Reactions with Nitric Oxide

symbol	electronic state	energy (au)	frequencies, cm^{-1} (intensities, km/mol)
N	^4S	−54.57537	
O	^3P	−75.05634	
Zr	^3F	−46.79981	
Hf	^3F	−48.6856	
NO	$^2\Pi$	−129.89948	1887(36)
ZrN	$^2\Sigma$	−101.62261	991(110)
ZrO	$^1\Sigma$	−122.15894	963(125)
HfN	$^2\Sigma$	−103.49823	942(26)
HfO	$^1\Sigma$	−124.07612	961(96)
NZrO	$^2A'$	−176.8933	a′ 853(73), a′ 686(56), a′ 221(11)
OZrO	$^1A_1$	−197.47473	a_1 890(35), b_2 828(275), a_1 305(6)
ZrNO	$^2\Pi$	−176.8346	σ 1555(718), σ 593(1), π 292(39 × 2)
Zr−η^2-NO	$^2A'$	−176.85917	a′ 880(77), a′ 680(14), a′ 458(1)
NHfO	$^2A'$	−178.77257	a′ 858(58), a′ 667(21), a′ 225(7)
OHfO	$^1A_1$	−199.35425	a_1 884(20), b_2 801(190), a_1 300(4)
HfNO	$^2\Pi$	−178.72216	σ 1548(362), σ 532(4), π 344(11 × 2)
Hf−η^2-NO	$^2A'$	−178.74563	a′ 847(55), a′ 704(6), a′ 418(1)
Hf(μ-N)(μ-O)Hf	$^2B_2$	−227.69985	a_1 774(11), b_2 687(310), a_1 636(57), b_2 493(30), a_1 240(1), b_1 158(9)

614.5, and 497.0 cm^{-1} in the Hf + $^{14}N^{16}O$ experiments and show isotopic splittings consistent with the vibrations of a single nitrogen atom (three doublets of bands at 654.3−652.1, 614.6−596.3, and 497.0−494.3 cm^{-1} in the $^{14}N^{16}O/^{15}N^{16}O$ experiments) and a single oxygen atom (three doublets of bands at 652.1−623.2, 596.2−594.7, and 494.3−469.7 cm^{-1} in the $^{15}N^{16}O/^{15}N^{18}O$ experiments). It is evident from the magnitudes of their isotopic shifts that both the highest and lowest frequency modes of this group are primarily Hf−O in character, while the highest intensity, middle frequency absorption is produced by a primarily Hf−N vibration. On the basis of the unusual frequency region for these modes and the fact that there appear to be two Hf−O vibrations in a one-oxygen-atom-containing species, it is likely that the molecule producing these spectra contains two Hf centers between which exists a bridging oxide ligand and perhaps a bridging nitride ligand as well. With this in mind, calculations were run on the planar dihafnium species Hf(μ-N)(μ-O)Hf.

BP86/AREP calculations on the C_{2v} Hf(μ-N)(μ-O)Hf species predict a $^2B_2$ electronic ground state where the bond between the N and the O in the di-η^2-bound nitric oxide species is completely cleaved in favor of the formation of the bridging oxide and nitride bonds. The harmonic frequencies produced by the present calculations predict that three of the six modes of this molecule produce infrared absorptions of sufficient intensity to be observed at 687, 636, and 493 cm^{-1} (Table 4). The calculated isotopic shifts indicate that the most intense absorption of this species, the mode at 687 cm^{-1}, should produce a 1.029 29 $^{14}N/^{15}N$ ratio that is in agreement with the ratio for the most intense observed absorption (614.5 cm^{-1} in the $^{14}N^{16}O$ experiments), which exhibits an analogous ratio of 1.030 69. Similar agreement is found between the isotope ratios for the other two observed modes of this species and the theoretically derived values. The $^{16}O/^{18}O$ isotope ratios of 1.046 95 and 1.050 74 for the DFT calculated modes at 636 and 493 cm^{-1}, respectively, when compared to the ratios of 1.046 37 and 1.052 37 for the observed absorptions at 654.3 and 495.0 cm^{-1}, provide excellent support for the present assignment. It is evident from the above discussion that the level of theory used in the present study is sufficient for the cursory analysis required within the scope of this work; however, the relative discrepancies in the calculated and observed vibrational frequencies for this species indicate that this molecule is pushing the limits of the presently applied quantum chemical methods.

Zirconium and Hafnium Nitrosyl Complexes in Solid Argon. As with the titanium nitrosyl stretching region, the assignment of zirconium and hafnium nitrosyl complexes is complicated by the unavoidable absorptions due to matrix-isolated water, NO_2, and $(NO)_2^+$. In addition, spectral interpretation in this region is further complicated by the tendency of the heavier η^1-bound group IV nitrosyl complexes to be relatively weak absorbers, exceedingly photosensitive, and highly dependent on the conditions of the initial co-deposition. Despite these shortcomings, it is possible to assign absorptions in the matrix spectra of reactions of Zr with $^{14}N^{16}O$ at 1598.7 and 1567.7 cm^{-1} and the broad multiple site split absorption at 1530.9 cm^{-1} to Zr−η^1-NO complexes. Analogous absorptions are observed at 1594.4, 1565.2, and 1519.7 cm^{-1} in the Hf + $^{14}N^{16}O$ experiments. In each case, the pure isotopic $^{14}N^{16}O$, $^{15}N^{16}O$, and $^{15}N^{18}O$ counterparts of the above bands are readily identifiable, as listed in Tables 1−3, but the important intermediate spectral features in the mixed $^{14}N^{16}O/^{15}N^{16}O$ and $^{15}N^{16}O/^{15}N^{18}O$ samples are impossible to discern, and these bands can therefore be assigned no more definitely than to generic M−η^1-$(NO)_x$ complexes.

DFT calculations performed on the Zr and Hf mononitrosyl complexes found that in both cases the linear $^2\Delta$ electronic state is the ground configuration. In addition, it must be noted that the geometry optimization of these species had to be constrained to a linear configuration because if the molecule were allowed to bend, the calculation would proceed to the metal insertion product, indicating the remarkable stability of the NMO species with respect to all other possible M(NO) conformations. The calculations predict that the N−O vibrations of the ZrNO and HfNO species should occur at 1555 and 1548 cm^{-1}, respectively, which suggests that the bands observed in the Zr and Hf experiments are in the proper spectral region to be due to the linear mononitrosyls. However, because of the lack of unambiguous data in the mixed isotopic experiments, no definite assignment can be made at this time.

Thorium Oxides. Because of the energetic nature of the laser-ablation process, atomization of the precursor is possible, and therefore, one must always be aware of pure oxide or pure nitride species in experiments with the nitrogen oxides.[40] Previous studies by Gablenick et al.[17] have provided absorptions for thorium oxides isolated in argon, but several experiments with thorium and oxygen were done to serve as a complement to the nitrogen oxide work. The results of both sets of experiments found that thorium monoxide and thorium dioxide are primary reaction products whether using O_2 or N_xO_y as the oxygen source. In these experiments, the site split absorptions at 876.3 (878.8) cm^{-1} in the ^{16}O experiments and 831.9 (829.6) cm^{-1}

in the ^{18}O-labeled experiments are due to the ThO molecule, in agreement with the previous work.[17]

Because of its well-documented C_{2v} bent structure,[17] the OThO molecule produces two infrared-active Th−O stretching modes. The symmetric (ν_1) vibration of OThO occurs at 787.3 cm^{-1} in the ^{16}O experiments and splits into a triplet of bands in mixed $^{16,18}O_2$ experiments: 787.3−772.7−743.8 cm^{-1}. The large $^{16}O/^{18}O$ ratio of 1.058 48 for this mode is consistent with a symmetric stretching mode. The antisymmetric Th−O stretching vibration (ν_3) appears at 735.0 cm^{-1} in the ^{16}O experiments and splits into a triplet of bands, 735.0−708.8−697.1 cm^{-1}, in the $^{16,18}O_2$ mixed isotope experiments. In comparison to the ν_1 mode, the ν_3 vibration exhibits a relatively small $^{16}O/^{18}O$ isotope ratio, 1.054 37. In the experiments with NO, in addition to the isolated OThO species, bands in the Th−O stretching region provide evidence for complexes of the OThO molecule. Upon matrix annealing, relatively intense bands grow in to the red of the absorptions associated with the ν_1 and ν_3 Th−O stretching modes of OThO. These modes are invariant with respect to nitrogen isotopic labeling. In both the $^{14}N^{16}O$ and $^{15}N^{16}O$ experiments, these two bands appear at 783.2 and 729.0 cm^{-1}. In the Th + $^{15}N^{16}O/^{15}N^{18}O$ and $^{14}N^{16}O/^{15}N^{18}O$ mixed oxygen experiments, these modes split into triplets in a manner analogous to the uncomplexed OThO modes: 783.2−768.3−739.9 and 729.0−703.2−691.4 cm^{-1}. As can be seen, these modes produce isotopic ratios almost identical to the ν_1 and ν_3 modes of the uncomplexed species, providing solid evidence that they are being produced by a perturbed OThO unit, most likely the molecular complex of generic form (OThO)(N_2) from the reaction of Th and $(NO)_2$.

Conclusions

Group IV metal atoms (Ti, Zr, and Hf) produced by laser-ablation react with nitric oxide on co-condensation with excess argon to form several new transient product species including the metal insertion products NMO (M = Ti, Zr, and Hf). These reactions are so favorable as to give a 3- to 4-fold increase in NMO bands on annealing to 21−24 K in solid argon. Bands at 900.6, 844.2, and 855.2 cm^{-1}, respectively, in the reactions of these metals with $^{14}N^{16}O$ are indicative of the Ti−O, Zr−O, and Hf−O stretching vibrations of these bent molecules (Figure 1). The associated M−N stretching coordinates occur at 718.2, 673.3, and 685.3 cm^{-1}, respectively. Scrutiny of the vibrational frequencies of these species bring to light some interesting and counterintuitive trends within the metals of group IV. As is expected, the vibrational frequencies of the M−O and M−N stretching modes of the insertion products decrease significantly from the Ti to the Zr products, consistent with the increase of mass between the titanium and zirconium metal centers; however, the analogous modes in the Hf species increase by an average of almost 10 cm^{-1} over the Zr product, which is in contrast to the expected frequency decrease in these vibrational coordinates as a result of the mass increase and shell expansion between Zr and Hf. Vibrational energy inversions of this nature have been observed in similar studies of the Zr and Hf oxides and hydrides.[41−43] This trend is, of course, not continued with NThO (760.3, 697.3 cm^{-1} stretching modes). The reversal between Zr and Hf can be associated with the increase in the relativistic effects felt by the atomic orbitals of s and p symmetries on the hafnium atom. Relativity in the heavier elements manifests itself in the energetic stabilization and spatial contraction of these orbitals, which in turn strengthens the bonding in hafnium-containing species with respect to the analogous zirconium species. Although often overlooked, it is becoming more evident through studies such as the present matrix isolation and analogous theoretical investigations that the unique chemistries associated with the second- and third-row transition elements are determined for the most part by the subtle atomic structural changes induced by relativistic orbital effects.[32]

Density functional calculations were performed and used as an additional basis for spectral interpretation and assignment. Special note should be given to the exceptional performance of the AREP's and associated basis sets used in the present work in conjunction with the BP86 functional for predicting vibrational frequencies of transition metal containing transients. Scale factors for these open-shell NZrO (0.989, 0.981) and NHfO (0.997, 1.027) molecules are in the range of values for pure density functionals.[44,45]

In addition to the metal-insertion product, NMO, the reactions of the cold metal atoms with the dimer of nitric oxide, $(NO)_2$, produce several new mixed nitride−oxide species of the group IV metals. When the matrix is annealed, the growth of bands in the mid-1400, high-1100, and high-800 cm^{-1} regions of all three metals co-deposited with NO provides evidence for the formation of an η^2-bound nitrous oxide complex of the metal monoxide. Other absorptions that grow as a result of matrix annealing are indicative of an O-bound nitrous oxide complex and a metal dioxide−molecular dinitrogen complex, both of which appear to be a progeny of cold metal atom reactions with $(NO)_2$.

Acknowledgment. We gratefully acknowledge support from the Air Force Office of Scientific Research.

References and Notes

(1) Ward, T. R.; Alemany, P.; Hoffman, R. *J. Phys. Chem.* **1993**, *97*, 7691.
(2) Cotton, F. A.; Wilkinson, G. *Advanced Inorganic Chemistry: A Comprehensive Text*, 5th ed.; Interscience Publishers: New York, 1988.
(3) Yamamoto, A. *Organotransition Metal Chemistry: Fundamental Concepts and Applications*; Wiley-Interscience: New York, 1986.
(4) Stryer, L. *Biochemistry*, 4th ed.; W. H. Freeman Publishers: New York, 1995.
(5) Wink, D. A.; Grisham, M. B.; Mitchell, J. B.; Ford, P. C. *Methods in Enzymology*; Academic Press: San Diego, 1996; Vol. 268.
(6) Culotta, E.; Koshland, D. E., Jr. *Science* **1992**, *258*, 1862.
(7) Verma, A.; Hirsch, D. J.; Glatt, C. E.; Ronnett, G. V.; Snyder, S. H. *Science* **1993**, *259*, 381.
(8) Rutherford, J. A.; Mathis, R. F.; Turner, B. R.; Vroom, D. A. *J. Chem. Phys.* **1972**, *56*, 4654; *J. Chem. Phys.* **1972**, *57*, 3091.
(9) Schlög, R. *Angew. Chem.* **1993**, *105*, 402.
(10) Andrews, L.; Chertihin, G. V.; Citra, A.; Neurock, M. *J. Phys. Chem.* **1996**, *100*, 11235.
(11) Zhou, M. F.; Andrews, L. *J. Phys. Chem. A* **1998**, *102*, 7452.
(12) Andrews, L.; Zhou, M. F.; Willson, S. P.; Kushto, G. P.; Snis, A.; Panas, I. *J. Chem. Phys.* **1998**, *109*, 177.
(13) Zhou, M. F.; Andrews, L. *J. Phys. Chem. A* **1998**, *102*, 10025.
(14) Zhou, M. F.; Andrews, L. *J. Phys. Chem. A* **1999**, *103*, 478.
(15) Kushto, G. P.; Zhou, M. F.; Andrews, L.; Bauschlicher, C. W., Jr. *J. Phys. Chem A* **1999**, *103*, 1115.
(16) Souter, P. F.; Kushto, G. P.; Andrews, L.; Neurock, M. *J. Phys. Chem. A* **1997**, *101*, 1287.
(17) Gabelnick, S. D.; Reedy, G. T.; Chasanov, M. G. *J. Chem. Phys.* **1974**, *60*, 1167 and references therein.
(18) Kushto, G. P.; Souter, P. F.; Andrews, L. *J. Chem. Phys.* **1998**, *108*, 7121.
(19) Tasumi, K.; Nakamura, A. *Inorg. Chem.* **1980**, *19*, 2656.
(20) Pyykkö, P.; Laakkonen, L. J.; Tatsumi, K. *Inorg. Chem.* **1989**, *28*, 1801.
(21) Pepper, M.; Bursten, B. E. *Chem. Rev.* **1991**, *91*, 719.
(22) Burkholder, T. R.; Andrews, L. *J. Chem. Phys.* **1991**, *95*, 8697.
(23) Hassanzadeh, P.; Andrews, L. *J. Phys. Chem.* **1992**, *96*, 9177.
(24) Frisch, M. J.; Trucks, G. W.; Schlegel, H. B.; Gill, P. M. W.; Johnson, B. G.; Robb, M. A.; Cheeseman, J. R.; Keith, T. A.; Petersson, G. A.; Montgomery, J. A.; Raghavachari, K.; Al-Laham, M. A.; Zakrzewski, V. G.; Ortiz, J. V.; Foresman, J. B.; Cioslowski, J.; Stefanov, B. B.; Nanayakara, A.; Challacombe, M.; Peng, C. Y.; Ayala, P. Y.; Chen, W.;

Wong, M. W.; Andres, J. L.; Replogle, E. S.; Gomperts, R.; Martin, R. L.; Fox, D. J.; Binkley, J. S.; Defrees, D. J.; Baker, J.; Stewart, J. P.; Head-Gordon, M.; Gonzales, C.; Pople, J. A. *GAUSSIAN 94*; Gaussian Inc.: Pittsburgh, PA, 1995.

(25) Becke, A. D. *Phys. Rev. A* **1988**, *38*, 3098.

(26) Perdew, J. P. *Phys. Rev. B* **1986**, *33*, 8822.

(27) LaJohn, L. A.; Christiansen, P. A.; Ross, R. B.; Atashroo, T.; Ermler, W. C. *J. Chem. Phys.* **1987**, *87*, 2812.

(28) Ross, R. B.; Powers, J. M.; Atashroo, T.; Ermler, W. C.; LaJohn, L. A.; Christiansen, P. A. *J. Chem. Phys.* **1990**, *93*, 6654.

(29) Young-Kyu, H. *J. Phys. Chem.* **1996**, *100*, 18004.

(30) Walch, S. P.; Bauschlicher, C. W., Jr.; Nelin, C. J. *J. Chem. Phys.* **1983**, *79*, 3600.

(31) Wittborn, C.; Wahlgren, U. *Chem. Phys.* **1995**, *201*, 357.

(32) Pyykkö, P. *Chem. Rev.* **1988**, *88*, 563.

(33) Kushto, G. P. Ph.D. Thesis, University of Virginia, Charlottesville, 1999. The 117.7° angle calculated by DFT(ADF) is in very good agreement with the 122.5° value from the 16/18 isotopic ratio (ν_3) and vibrational analysis (ref 17).

(34) Andrews, L.; Bare, W. D.; Chertihin, G. V. *J. Phys. Chem. A* **1997**, *101*, 8417.

(35) Chertihin, G. V.; Andrews, L.; Bauschlicher, C. W., Jr. *J. Am. Chem. Soc.* **1998**, *120*, 3205.

(36) Chertihin, G. V.; Bare, W. D.; Andrews, L. *J. Phys. Chem. A* **1998**, *102*, 3967.

(37) Kushto, G. P.; Souter, P. F.; Chertihin, G. V.; Andrews, L. *J. Chem. Phys.*, in press.

(38) Blomberg, M. R. A.; Siegbahn, P. E. M. *J. Am. Chem. Soc.* **1993**, *115*, 6908.

(39) Chertihin, G. V.; Andrews, L. *J. Phys. Chem.* **1994**, *98*, 5891.

(40) Kushto, G. P.; Souter, P. F.; Andrews, L.; Neurock, M. *J. Chem. Phys.* **1997**, *106*, 5894.

(41) Chertihin, G. V.; Andrews, L. *J. Phys. Chem.* **1995**, *99*, 6356.

(42) Chertihin, G. V.; Andrews, L. *J. Am. Chem. Soc.* **1995**, *117*, 6402.

(43) Chertihin, G. V.; Andrews, L. *J. Phys. Chem.* **1995**, *99*, 15004.

(44) Scott, A. P.; Radom, L. *J. Phys. Chem.* **1996**, *100*, 16502.

(45) Bytheway, I.; Wong, M. W. *Chem. Phys. Lett.* **1998**, *282*, 219.